Metal selective co-ordinative self-assembly of π-donors

ANKIT JAIN, K VENKATA RAO, ANKITA GOSWAMI and SUBI J GEORGE*

Supramolecular Chemistry Laboratory, New Chemistry Unit, Jawaharlal Nehru Centre for Advanced
Scientific Research, Jakkur, Bangalore 560064, India
e-mail: george@jncasr.ac.in

Abstract.   Metal selective co-ordinative nanostructures were constructed by the supramolecular co-assembly of pyridine appended TTF (**TTF-Py**) and pyrene (**PYR-Py**) derivatives in appropriate solvent composition mixtures with metal ions. Microscopic analyses show that **TTF-Py** shows distinctive morphology with either of these metal ions, forming I-D tapes with 1:1 Pb^{2+} complex and 2-D sheets with 1:2 Zn^{2+} complex. A rationale has been provided from molecular level packing for such hierarchical changes. In case of Cu^{2+}, we have observed an anomalous binding of metal ion to the core sulphur groups causing redox changes in the TTF core. **PYR-Py** on the other hand is shown to be a fluorescent sensor for Pb^{2+}, Zn^{2+}, Hg^{2+} and Ag^+. With different fluorescent response for metal complexes, we essentially obtained similar 1-D assemblies suggesting similar binding modes for all of them. Supramolecular approach through which morphology of an electron donor moiety can be engineered by metal ions can be a new tool in nanoelectronics.

Keywords.   Self-assembly; π-donor molecules; nanostructures; metal ion sensing.

1.   Introduction

Molecular self-assembly based on rational control of non-covalent interactions such as hydrophobic interactions, hydrogen bonding, aromatic stacking and/or metal coordination interactions, provides powerful bottom-up tools for the design of hierarchical structures of nano- to micrometer scale.[1] Molecular and supramolecular electronics is one of the most important applications of nano assemblies.[2] From the point of view of nanosized organic electronics, assembly of electron-rich molecules i.e., π-donor is of quite significance.[3] A plethora of π-donor systems have been already shown to be self-assembling using the aid of various non-covalent interactions such as H-bonding and π–π stacking.[4] On the other hand, coordination polymers of metal ions with the organic ligands can result in interesting structures such as spherical particles,[5] rigid rods,[6] nanotubes[7] and springs[8] of micro to even nano dimension. However, there are only a few reports of metal-induced solution phase self assembly of electronically active molecules and more efforts to realize self assembly of π-donor systems which are selective to metal ions are required.[9]

Here, we report the synthesis of two π-donors, tetrathiafulvalene (TTF) and pyrene, appended with pyridine ligand (scheme 1) and their coordination morphologies with various metal ions. TTF is one of the most extensively studied moieties for molecular electronics.[10] Various fibrous self-assembling derivatives of TTF have been reported using H-bonding interactions which not only can be used as semiconducting wires but also give insights into the self-assembly characteristics of molecules with TTF as the active π surface.[11] Using intermolecular non-covalent interactions to build TTF-based self-assemblies is a fascinating subject even though the construction of nanostructures that behave as a conductor is still a daunting task. Recently Wu *et al*. has reported metal-induced morphologies of dipyridyl derivative of TTF.[9] Pyrene moieties on the other hand, have been the focus of much photo-physical investigation due to the higher frequency fluorescence, this chromophore imparts to the molecules. In addition, pyrene-based assemblies have been achieved by means of H-bonding and charge transfer interactions.[12] Here we chose pyrene because it gave more spectroscopic flexibility as its photoluminescence could also be monitored.

Thus, in the present work we have focussed our attention on metal-assisted co-ordinative self-assembly of electron-rich TTF pyridine derivative **TTF-Py** and

---

*For correspondence
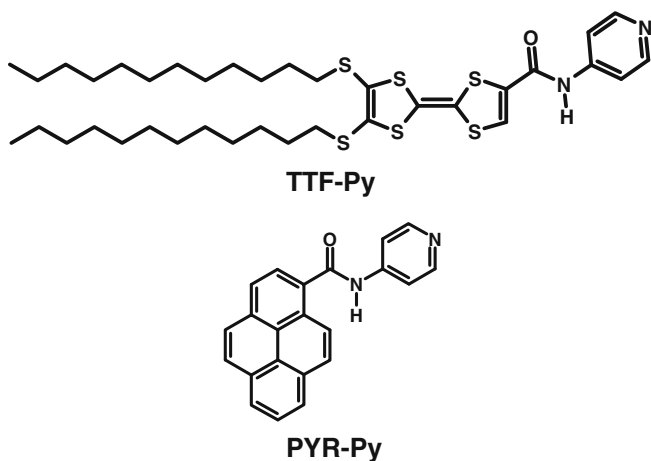
TTF-Py

PYR-Py

Scheme 1. Schematic representation of the chromophores under study: **TTF-Py**, **PYR-Py**.

pyrene pyridine derivative **PYR-Py** (scheme 1). We have rendered these π-donors with pyridine functionality in order to promote the co-ordination with metal ions. Furthermore, the chromophores are functionalized with amide groups for giving directionality to the π-stacked assembly of metal co-ordinated ligands via H-bonding (scheme 2). The synchronized properties bestowed upon it by the π-π interaction of the aromatic domain, hydrogen bonding by the amide moiety, hydrophobic interactions by the long alkyl chains

and finally by the metal ion induced orientation can form extended nanoscale assemblies as shown in the schematic (scheme 2).

2. Experimental

2.1 *Synthesis and experimental procedures*

TTF-Py and **PYR-Py** were synthesized according to scheme 3. 2,3-*Bis*(dodecylthio)-6-(carboxy) tetrathiafulvalene (**1**) was synthesized according to literature procedure.[13] **1** was then converted to the acid chloride (**1a**) using oxalylchloride and subsequent amidation with 4-amino pyridine yielded the **TTF-Py**. Similarly, the pyrene acid (**2**) was converted to its acid chloride (**2a**) and subjected to amidation to obtain **PYR-Py**. Both the derivatives have been characterized fully by various analytical techniques such as ^{1}H-NMR and MALDI-TOF.

2.1a *2,3-Bis(dodecylthio)-6-(carboxy)tetrathiafulvalene (1)*: To a solution of 2,3-*Bis*(dodecylthio)-6-(methoxycarbonyl)tetrathiafulvalene[13] (240 mg, 0.36 mmoles) in THF (26.5 ml), LiOH (111 mg) in H_2O (5 ml) was added drop-by-drop and the mixture was stirred at room temperature for 12 h. After the reaction was over, to the mixture 30 ml of diethyl ether
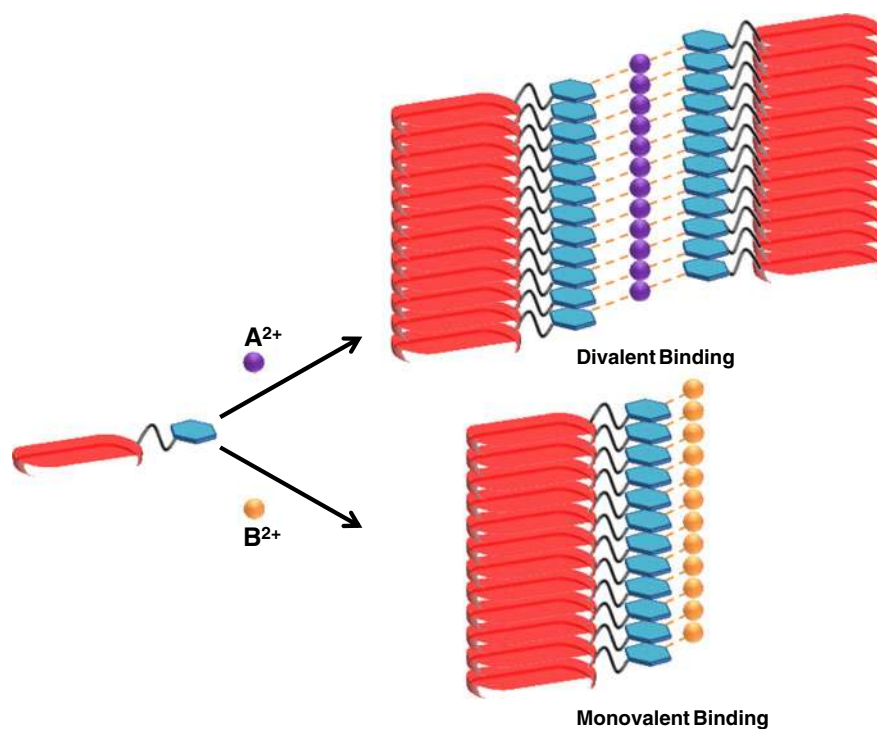
Scheme 2. Schematic representation of metal-directed self-assembly of the chromophores with mono and divalent binding is shown.
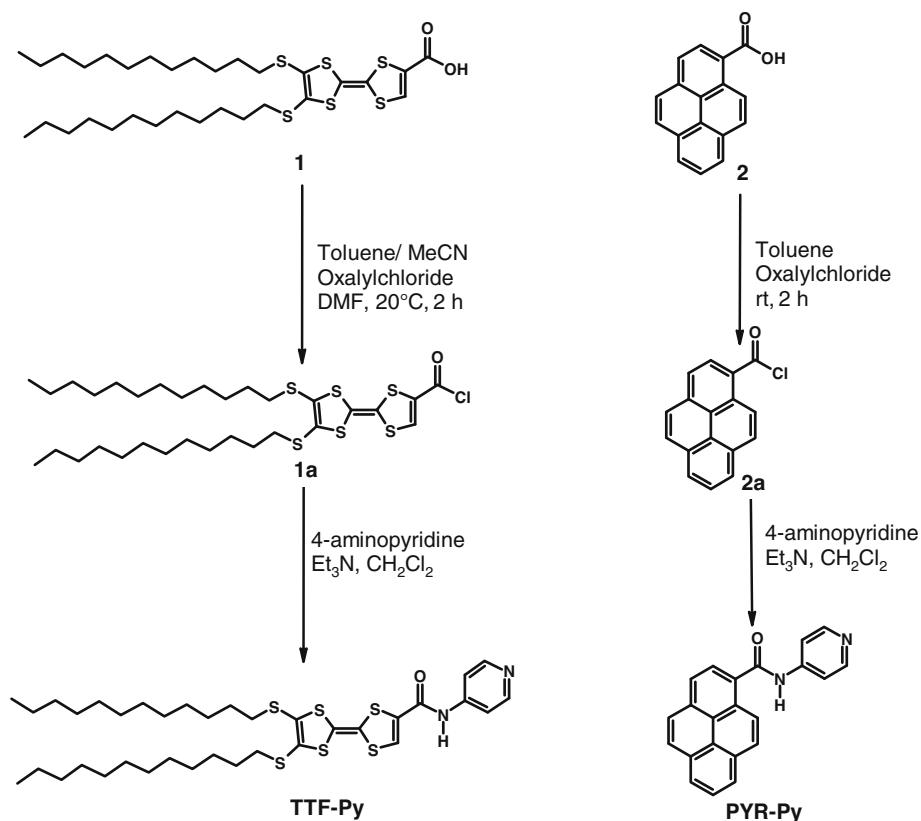
Scheme 3. Synthetic scheme followed for the synthesis of **TTF-Py** and **PYR-Py**.

is added. This is subsequently acidified by 30 ml of 0.5 M HCl solution. The organic layer is separated and evaporated to dryness. The reaction mixture was further purified by column chromatography (20% MeOH in DCM), yielding 220 mg of compound (yield 94%). MALDI-TOF/MS $m/z(\%)$: 648.34 [M+]; calculated for $C_{31}H_{52}S_6O_2$, 649.14 gmol^{-1}. ^{1}H NMR (CDCl$_3$): 6.98 (s, C=CH, 1H), 2.27 (t, S-CH$_2$, 4H), 1.42 (m, S-CH$_2$CH$_2$, 4H), 1.22–1.25 (m, -S-(CH)$_2$CH$_2$ 36H), 0.88 (t, CH$_3$, 6H) ppm.

2.1b *Synthesis of 2,3-Bis(dodecylthio)-6-(acetylchloride)tetrathiafulvalene (1a)*: To a solution of 2,3-*Bis*(dodecylthio)-6-(carboxy)tetrathiafulvalene **(1)** (200 mg, 0.301 mmol) in toluene/MeCN (14 ml; 5:1 ratio), were added oxalylchloride (0.028 ml, 0.331 mmol) and DMF (1 drop of a 10% solution in toluene) and the solution was stirred for 2 h at 20°C. The reaction mixture was filtered through a pad of dry silica gel (1 cm) and neutral alumina. The filter was washed with toluene, and the filtrate was evaporated under *vacuum* yielding **1a** (150 mg, 72%) as dark red oil, which was used without further purification.

2.1c *Synthesis of pyridine appended TTF (TTF-Py)*: To an ice cooled solution of 4-aminopyridine (20 mg, 0.22 mmol) and triethylamine (0.092 ml, 0.66 mmol) in dry THF (4 ml), solution of **1a** in dry dichloromethane (DCM) (10 mL) was added drop-wise. Stirring was continued for another 1 h at 0°C and then at room temperature for overnight. The above solution was diluted with DCM and washed with water (2 times) and then brine. The solution was dried over Na$_2$SO$_4$ and evaporated *in vacuo* to get a dark red solid, which was further purified by column chromatography (6% MeOH in DCM), yielding 60 mg (yield 37.7%) of **(TTF-Py)**. MALDI-TOF/MS $m/z(\%)$: 724.4 [M+]; calculated for $C_{36}H_{56}S_6N_2O$, 724.12 gmol^{-1}. ^{1}H NMR (CDCl$_3$): 8.54 (d, Py-H, 2H), 7.5 (d, Py-H, 2H), 7.44 (s, CONH, 1H), 7.3 (s, C=CH, 1H), 2.82 (t, S-CH$_2$, 4H), 1.63 (m, S-CH$_2$CH$_2$, 4H), 1.25–1.43 (m, -S-(CH)$_2$CH$_2$ 36H), 0.89 (t, CH$_3$, 6H) ppm.

2.1d *Synthesis of pyrene acid chloride (2a)*: To a solution of **2** (100 mg, 0.406 mmol) in 5 ml toluene, 1.1 equivalent of oxalylchloride was added drop-wise and the reaction was refluxed for 2 h. After 2 h the solvent was evaporated and yellow colour solid was

obtained which was used for next step without further purification.

2.1e *Synthesis of pyridine appended pyrene (PYR-Py)*: To a solution of 4-aminopyridine (84 mg, 0.89 mmol) and triethylamine (0.37 ml, 2.67 mmol) in dry dichloromethane (4 ml), dispersion of **2a** in dry dichloromethane (10 mL) was added drop-wise. Stirring was continued for another 6 h at room temperature. The above solution was diluted with DCM and washed with water (2 times) and then brine. The solution was dried over Na_2SO_4 and evaporated *in vacuo* to get a light yellow solid, which was further purified by column chromatography (5% MeOH/CHCl$_3$), yielding 104 mg (yield 80%) of **PYR-Py.** MALDI-TOF/MS m/z(%): 323.00 [M+]; calculated for $C_{22}H_{14}N_2O$, 322.37 gmol^{-1}. ^{1}H NMR (CDCl$_3$): 8.59 (m, 3H), 8.27 (d, 2H), 8.19 (m, 4H), 8.085 (m, 3H), 7.7 (d, 2H) ppm.

2.2 *General methods*

^{1}H NMR was recorded on Bruker AVANCE-400 MHz spectrometer at room temperature. FE-SEM measurements were performed on NOVA NANO SEM 600 (FEI) operated at 15 kV, by drop casting the solution on glass substrate. Some of the samples were recorded with gold sputtering and some of them recorded in low vacuum mode. TEM measurements were performed on a JEOL, JEM 3010 operated at 300 kV. Samples were prepared by placing a drop of the solution on carbon-coated copper grids followed by drying at room temperature. In order to get a better contrast, some samples were stained with uranyl acetate (1 wt% in water) before the measurements. Electronic absorption spectra were recorded on Perkin Elmer Lambda 900 UV-Vis-NIR Spectrometer. UV-Vis spectra were recorded in 3 mm and 1 mm path length quartz cuvettes. Photoluminescence (PL) spectra were recorded with a Perkin-Elmer model LS55 luminescence spectrometer. MALDI-TOF spectra were obtained on a Bruker ultraflex-2 MALDI-TOF mass spectrometer with α-cyano-4-hydroxycinnamic acid as the matrix.

3. Results and discussion

We have first studied the absorption properties of **TTF-Py** in hexane (c = 10^{-5} M) to probe its self-assembly behaviour which showed an intramolecular charge transfer band around 450 nm, characteristic of charge transfer between the HOMO of TTF and the LUMO of pyridyl moiety.[9] Interestingly, the CT band around 450 nm and local electronic transition bands around 280 nm showed a bathochromic shift as the concentration increases suggesting concentration dependent aggregation in hexane (figure 1a). FE–SEM images of the aggregated solution drop-casted on glass substrate show a network of fibres reiterating the self-assembly process (figure 1b). Aggregation was further evident from the gelation of these systems at higher concentrations (CGC in hexane = 27.6 mM). However, this critical aggregation concentration value is higher than that of the amide and urea appended TTF based gelators reported in literature[11] probably because of weak π–π stacking interactions resulting from the twisting of chromophores and hence reducing the effective π–π overlap surface. Thus, we further supported the H-bonding with metal ligand co-ordination to induce effective self-assembly (*vide infra*).
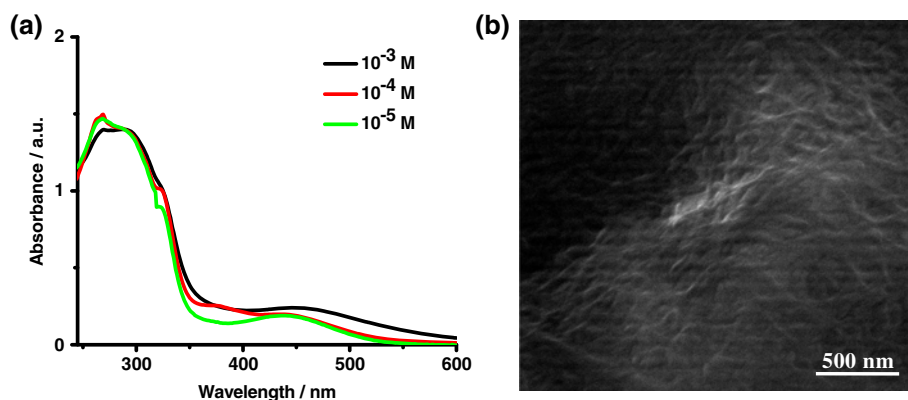

Figure 1. (**a**) Concentration dependent UV-Vis spectra of **TTF-Py** (normalized at 300 nm) in hexane and (**b**) FE-SEM image of 10^{-3} M **TTF-Py** drop casted on glass substrate.

We have first studied the co-ordination of various metal ions to the **TTF-Py** in 1:1 MeCN-CHCl$_3$ solvent mixture, chloroform to molecularly dissolve TTF and MeCN for the solubility of metal perchlorates. To elaborate, when a metal ion binds to ligand i.e., in this case pyridine, there is a red shift in the CT band upon complexation, the effect which can be seen visibly by a colour change. The red shifts in the CT band can be explained by the fact that as complexation occurs, it increases the electron accepting ability of the pyridyl, hence decreasing the LUMO of the molecule.[9] To achieve metal ion-induced structures, we need to choose metal ions which have higher charge transfer stabilization with lowest possible concentration of ions, i.e., metal ions with high selectivity of binding towards the chromophores. Interestingly, from the various metal ions such as K$^+$, Cd^{2+}, Zn^{2+}, Ba^{2+}, Ag$^+$, Hg^{2+}, Pb^{2+}, Mg^{2+} and Cu^{2+} the ones that produced maximum changes were Zn^{2+}, Pb^{2+} and Cu^{2+}. It is evident from the UV spectra and the concentration plots of various metal ions that **TTF-Py** was most sensitive for Zn^{2+} and Pb^{2+} (figure 2a).

There was a visible difference in the colour produced by the interactions of these metal ions with **TTF-Py** as Pb^{2+} and Zn^{2+} gave dark red colour as soon as

introduced in a solution of **TTF-Py** (figure 2c). To our surprise, Cu^{2+} presented a special case in which it was found to be more sensitive for the sulphur atoms present at the core of **TTF-Py**. This differentiation with respect to Cu^{2+} was proven with the fact that it was also found to be binding to the TTF derivatives even without the pyridine functionality, such as the tetra-dodecyl substituted TTF derivative,[14] which was lacking in pyridine ligand. A visible colour change from yellow to red was observed as the equivalents of copper ion were increased from one to four. With higher excess of copper ion ($\sim$ 4–10 times excess) a deep blue colour appeared which vanished over a day on standing, which is probably due to quenching of the di-cationic species. Absorption studies of this phenomenon showed the presence of TTF radical cation (400–500 nm and broad band around 800 nm) at low equivalents (1–4 equiv.) of Cu^{2+} and a di-cation at higher equivalents (broad band around 650 nm) (more than 4 equiv.)[15] (figure 2b). The above observation makes TTF derivative **TTF-Py** a visible sensor for metals such as Pb^{2+}, Zn^{2+} and Cu^{2+} (figure 2c).

Having established the selectivity in metal binding we have done detailed titration study in order to find out the mode of co-ordination and stoichiometry with
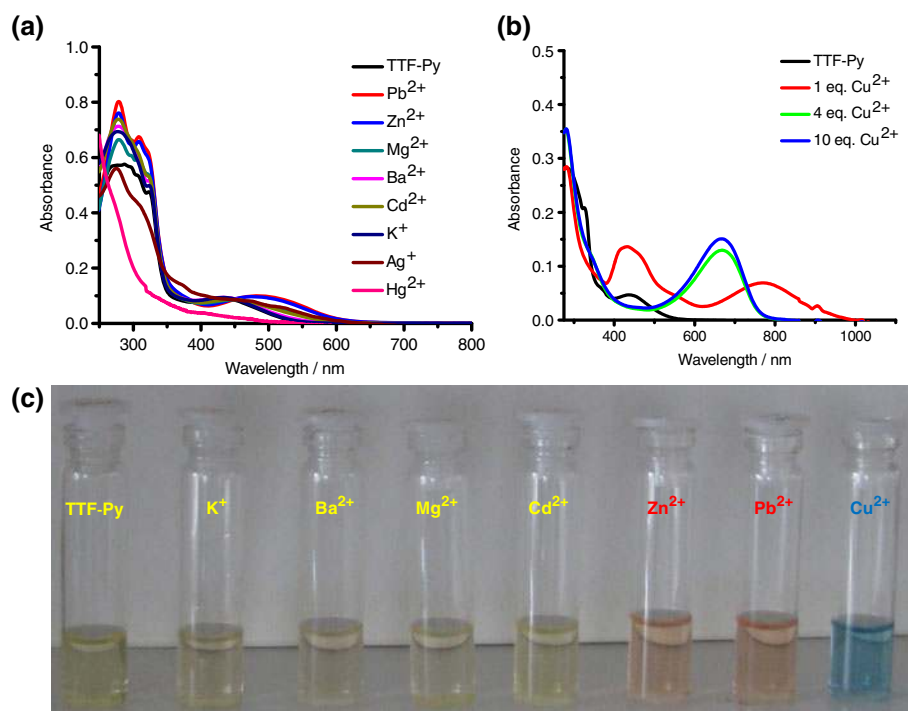

Figure 2. (**a**) UV-Vis spectra of 1:1 metal co-ordination with 10^{-4} M **TTF-Py** in 1:1 CHCl$_3$: MeCN, (**b**) UV-Vis spectra of different equivalents of Cu^{2+} co-ordination with 5×10^{-5} M **TTF-Py** in 1:1 CHCl$_3$: MeCN and (**c**) photographs showing visual changes of metal ion addition on **TTF-Py**.
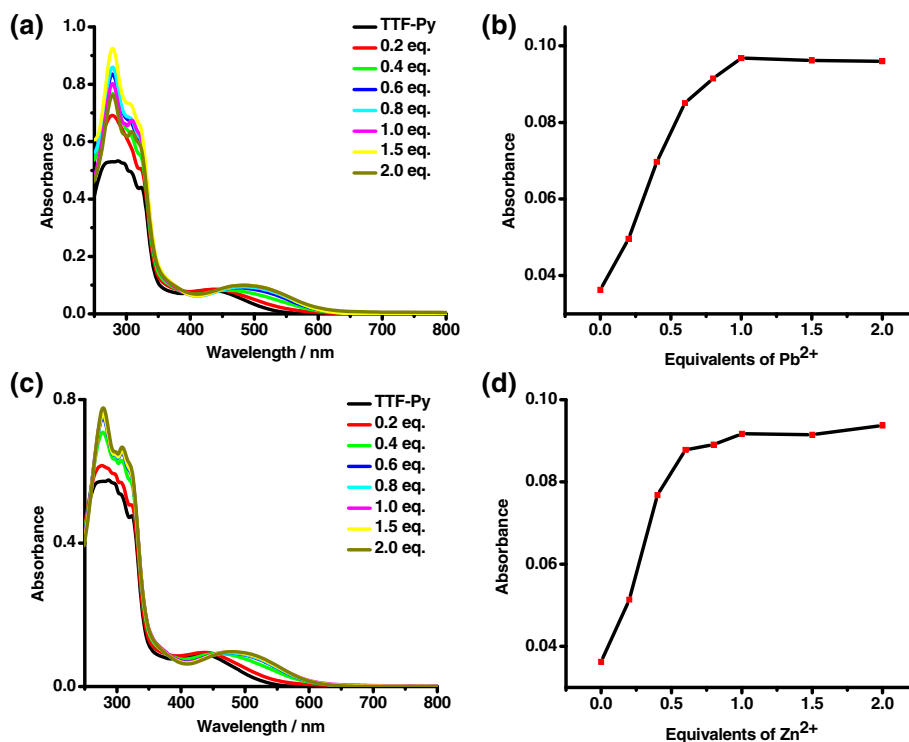
Figure 3. (**a**) UV-Vis spectra of various equivalents of Pb^{2+} titrated with **TTF-Py**, (10^{-4} M, in 1:1 $CHCl_3$:MeCN), (**b**) plot of equivalents of Pb^{2+} *vs* absorbance of the conjugate at 500 nm, (**c**) UV-Vis spectra of various equivalents of Zn^{2+} titrated with **TTF-Py**, (10^{-4} M, in 1:1 $CHCl_3$:MeCN) and (**d**) plot of equivalents of Zn^{2+} *vs* absorbance of the conjugate at 500 nm.
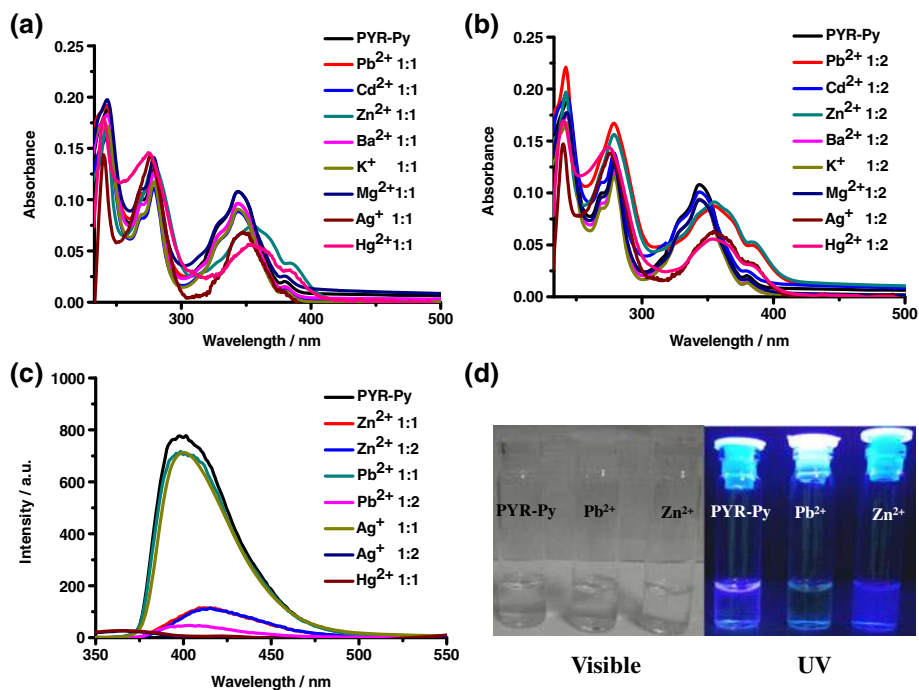

Figure 4. (**a, b**) UV-Vis spectra of **PYR-Py,** 10^{-5} M in MeCN with various metal ions at 1:1 and 1:2 equivalents respectively, (**c**) PL spectra of **PYR-Py,** 10^{-5} M in MeCN excited at 350 nm and (**d**) photograph showing visual changes to **PYR-Py** on addition of metal ions.

the more selective Pb^{2+} and Zn^{2+} ions. Thus based on the above observations, choice of metal ions was made, also a plot between equivalents of metal ion and the respective absorbance at 500 nm, coordination number based on the saturation of CT stabilization was proved to be 2:1 for Zn^{2+} and 1:1 for Pb^{2+} (figure 3). Mono-valent and di-valent binding was envisaged as in scheme 1, with di-valent being more extended in nature as compared to higher aspect ratio mono-valent binding (scheme 1).

Metal binding studies with **PYR-Py** were carried out in pure MeCN (10^{-5} M) as the ligand was found to be molecularly dissolved in this solvent. At this concentration **PYR-Py** is not aggregated though when it interacts with metal ions aggregates start to precipitate out on standing, hinting towards a spontaneous metal-induced self-assembly. **PYR-Py** was also found to be more sensitive for Pb^{2+}, Zn^{2+}, Hg^{2+} and Ag^+. As evident from figure 4, with one equivalents of the Zn^{2+} and Hg^{2+} **PYR-Py** absorption band around 343 nm showed a red shift of around 12 nm with concomitant quenching in the fluorescence. Similar red shift in the absorption

spectra and fluorescence quenching with Pb^{2+} and Ag^+ could only be seen when 2 equivalents of the metal ion was added. However, the absorption spectra had similar changes compared to that of Zn^{2+} and Hg^{2+}. We envisage that stoichiometrically the co-ordination number based on the titrations with metal ion equivalents for these four metal ions is actually 1:1 which is evident in case of Zn^{2+} and Hg^{2+}. In case of Pb^{2+} and Ag^+ however probably due to less association constants 1:1 binding is not translated in the titration studies and requires higher equivalents of metal ions for the saturation of binding sites.

Various nano structures could be induced from **TTF-Py** by metal ions through controlled interactions. The method that we used here to bring about steady state interaction was solvent diffusion. An acetonitrile solution of the metal per chlorates (5×10^{-4} M, 0.5 ml) was layered over the chloroform solution of **TTF-Py** (10^{-3} M, 0.5 ml). The layers were allowed to diffuse for 7 days, and various morphology studies were done on the samples. One curious observation worth mentioning is the formation of purple flaky structures especially in
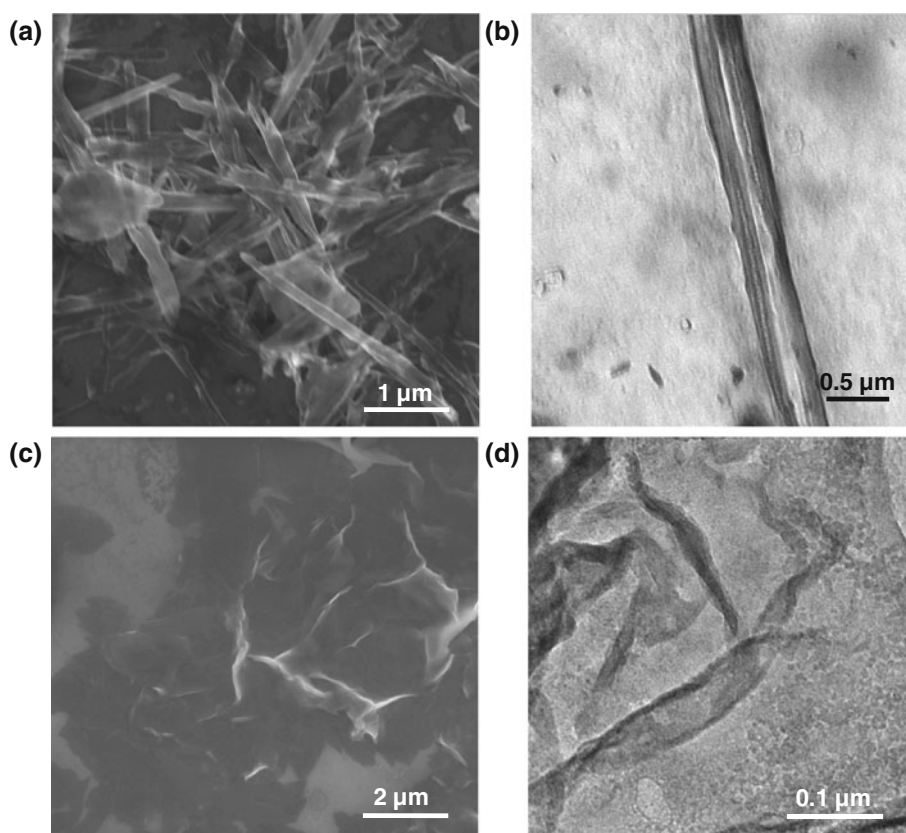

Figure 5. (**a, b**) FE-SEM and TEM images of 10^{-4} M solution of 1:1 **TTF-Py**: Pb^{2+} respectively, (**c, d**) FE-SEM and TEM images of 10^{-4} M solution of 1:2 **TTF-Py**: Zn^{2+}, respectively.
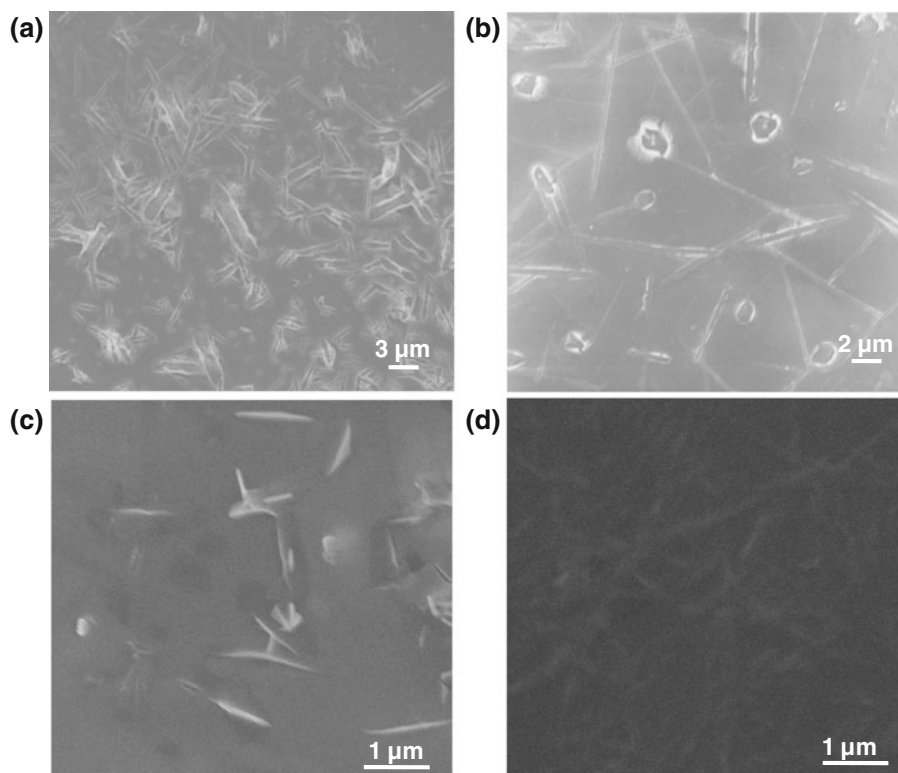
Figure 6. SEM images of (**a**) 10^{-4} M solution of 1:2 **PYR-Py**: Ag$^+$, (**b**) 10^{-4} M 1:1 **PYR-Py**: Hg^{2+} solution, (**c**) 10^{-4} M solution of 1:2 **PYR-Py**: Pb^{2+} and (**d**) 10^{-4} M 1:1 **PYR-Py**: Zn^{2+} solution. Experiments were carried out on a glass substrate.

case of Pb^{+2}. This could be attributed to be a giant supra molecularly self-assembled structure. We could observe the formation of tape-like, one-dimensional nano structure with Pb^{+2} of width distribution between 120 and 400 nm from the FE-SEM and TEM (figure 5a, b). With Zn^{2+} we could observe the formation of two-dimensional sheets. This was confirmed by FE-SEM and TEM (figure 5c, d).

Though the amorphous nature of the sample marred our attempts to study exact packing structure, but the results could be explained by the coordination number as shown earlier. Morphology results can be explained by the metal binding as shown in scheme 1. For Pb^{2+} since the molecular packing has length-wise growing incentive, morphology with higher aspect ratio of nanostructures is expected (scheme 2). However, In case of Zn^{2+} the packing can extend in a 2-D regime as the hydrophobic interactions between the alkyl chains transcend their effect on the morphology thus, explaining the 2D sheets.

SEM analysis of **PYR-Py** samples was done by aging the metal conjugated samples overnight. It could be seen that with Pb^{2+}, Zn^{2+}, Hg^{2+} and Ag$^+$**PYR-Py** shows essentially 1-D structures (figure 6) reiterating the 1:1 common binding model.

4. Conclusion

We have tried to bring out the versatility of metal-induced self-assembly in arranging π-donors such as **TTF-Py** and **PYR-Py** in different fashion. The molecular packing in **TTF-Py** metal conjugates transcends in its supramolecular morphology giving tapes and sheets for Pb^{2+} and Zn^{2+} respectively. We have also observed a deviation of behaviour of Cu^{+2} ions as they bind to the sulphur centre of the molecules in case of **TTF-Py**, thus making it an efficient sensor for Pb^{2+}, Zn^{2+} and Cu^{2+}. **PYR-Py** on the other hand was proved to be a fluorescent sensor for Pb^{2+}, Zn^{2+}, Hg^{2+} and Ag$^+$ with unique morphology. These hybrid nanostructures might be of potential use as conductive materials in nanoelectronics.

References

1. (a) Ajayaghosh A, George S J and Schenning A P H J 2005 in *Topics in current chemistry*, vol. 258, (Ed: F Würthner), Springer, pp. 83; (b) Babu S S, Kartha K K and Ajayaghosh A 2010 *J. Phys. Chem. Lett.* **1** 3413; (c) Ajayaghosh A, Praveen V K 2007 *Acc. Chem. Res.* **40** 644

2. (a) Brunsveld L, Folmer B J B, Meijer E W and Sijbesma R P 2001 *Chem. Rev.* **101** 4071; (b) Whitesides G M, Mathias J P and Seto C T 1991 *Science* **254** 1312; (c) Prins L J, Reinhoudt D N and Timmerman P 2001 *Angew. Chem., Int. Ed.* **40** 2382; (d) Shimizu T, Masuda M and Minamikawa H 2005 *Chem. Rev.* **105** 1401; (e) Yan Q, Yiyang L, Yijie W, Zhiyi Y, Jun L, Jiang Z, Yun Y and Jianbin H 2009 *Nano Lett.* **9** 4500

3. (a) Schoonbeek F S, van Esch J, Wegewijs B, Rep D B A, de Haas M P, Klapwijk T M, Kellogg R M and Feringa B L 1999 *Angew. Chem., Int. Ed.* **38** 1393; (b) Swager T M, Gil C J and Wrighton M S 1995 *J. Phys. Chem.* **99** 4886

4. (a) George S J and Ajayaghosh A 2001 *J. Am. Chem. Soc.* **123** 5148; (b) George S J and Ajayaghosh A 2005 *Chem. Eur. J.* **11** 3217; (c) Babu P, Sangeetha N M, Vijaykumar P, Maitra U, Rissanen K and Raju A R 2003 *Chem. Eur. J.* **9** 1922; (d) Hoeben F J M, Jonkheijm P, Meijer E W and Schenning A P H J 2005 *Chem. Rev.* **105** 1491; (e) Samanta S K, Pal A and Bhattacharya S 2009 *Langmuir* **25** 8567; (f) Bhattacharya S and Samanta S K 2009 *Langmuir* **25** 8378; (g) Prasanthkumar S, Saeki A, Seki S and Ajayaghosh A 2010 *J. Am. Chem. Soc.* **132** 8866; (h) Prasanthkumar S, Gopal A and Ajayaghosh A 2010 *J. Am. Chem. Soc.* **132** 13206; (i) Ajayaghosh A, Varghese R, Praveen V K and Mahesh S 2006 *Angew. Chem. Int. Ed.* **45** 3261; (j) Yagai S, Mahesh S, Kikkawa Y, Unoike K, Karatsu T, Kitamura A and Ajayaghosh A 2008 *Angew. Chem.* **120** 4769

5. (a) Oh M and Mirkin C A 2005 *Nature* **438** 651; (b) Sun X, Dong S and Wang E 2005 *J. Am. Chem. Soc.* **127** 13102; (c) Oh M and Mirkin C A 2006 *Angew. Chem., Int. Ed.* **118** 5618; (d) Maeda H, Hasegawa M, Hashimoto T, Kakimoto T, Nishio S and Nakanishi T 2006 *J. Am. Chem. Soc.* **128** 10024

6. (a) Würthner F, Stepanenko V and Sautter A 2006 *Angew. Chem., Int. Ed.* **118** 1973; (b) Jeon Y-M, Heo J and Mirkin C A 2007 *J. Am. Chem. Soc.* **129** 7480

7. (a) Kim Y, Mayer M F and Zimmerman S C 2003 *Angew. Chem., Int. Ed.* **115** 1153; (b) Liu B, Qian D-J, Chen M, Wakayama T, Nakamura C and Miyake J 2006 *Chem. Commun.* **30** 3175

8. Kim H-J, Lee E, Park H-S, Lee M 2007 *J. Am. Chem. Soc.* **129** 10994

9. (a) Geng Y, Wang X-J, Chen B, Xue H, Zhao Y-P, Lee S, Tung C-H and Wu L-Z 2009 *Chem. Eur. J.* **15** 51241; (b) Xue H, Tang X-J, Wu L-Z, Zhang L-P and Tung C-H 2005 *J. Org. Chem.* **70** 9727; (c) Ajayaghosh A, Chithra P, Varghese R 2007 *Angew. Chem., Int. Ed.* **46** 230; (d) Ajayaghosh A, Chithra P, Varghese R and Divya K P 2008 *Chem. Commun.* **8** 969; (e) Sreejith S, Divya K P and Ajayaghosh A 2008 *Chem. Commun.* **25** 2903; (f) Chithra P, Varghese R, Divya K P and Ajayaghosh A 2008 *Chem. Asian J.* **3** 1365

10. (a) Wang J–Y, Yan J, Ding L, Ma Y and Pei J 2009 *Adv. Funct. Mater.* **19** 1746; (b) Kitamura T, Nakaso S, Mizoshita N, Tochigi Y, Shimomura T, Moriyama M and Kato T 2005 *J. Am. Chem. Soc.* **127** 14769; (c) Luis Puigmarti J, Laukhin V, del Pino Á P, Gancendo J V, Rovira C, Laukhina E and Amabilino D B 2007 *Angew. Chem. Int. Ed.* **46** 238; (d) Danila I, Riobé F, Luis J P–, del Pino Á P, Wallis J D, Amabilino D B and Avarvari N 2009 *J. Mater. Chem.* **19** 4495; (e) Tatewaki Y, Hatanaka T, Tsunashima R, Nakamura T, Kimura M and Shirai H 2009 *Chem. Asian J.* **4** 1474; (f) Mukhopadhyay P, Iwashita Y, Shirakawa M, Kawano S–i, Fujita N and Shinkai S 2006 *Angew. Chem. Int. Ed.* **45** 1592; (g) Xiao J, Yin Z, Li H, Zhang Q, Boey F, Zhang H and Zhang Q J 2010 *J. Am. Chem. Soc.* **132** 6926

11. (a) Kitahara T, Shirakawa M, Kawano S, Beginn U, Fujita N and Shinkai S 2005 *J. Am. Chem. Soc.* **127** 14980; (b) Wang C, Zhang D and Zhu D 2005 *J. Am. Chem. Soc.* **127** 16372

12. (a) Wang C, Guo Y, Wang Y, Xu H, Wang R and Zhang X 2009 *Angew. Chem. Int. Ed.* **48** 8962; (b) Wang C, Yin S, Chen S, Xu H, Wang Z and Zhang X 2008 *Angew. Chem. Int. Ed.* **47** 9049; (c) Das R K, Kandanelli R, Linnanto J, Bose K and Maitra U 2010 *Langmuir* **26** 16141

13. (a) Green D C 1979 *J. Org. Chem.* **44** 1476; (b) Blanchard P, Salle M, Duguay G, Jubault M and Gorgues A 1992 *Tetrahedron Lett.* **33** 2685; (c) Gorgues A Hudhomme P and Salle M 2004 *Chem. Rev.* **104** 5151

14. Abdel–Mottaleb M M S, Gomar–Nadal E, Surin M, Uji–i H, Mamdouh W, Veciana J, Lemaur V, Rovira C, Cornil J, Lazzaroni R, Amabilino D B, De Feyter S and De Schryver F C 2005 *J. Mater. Chem.* **15** 4601

15. Xu C-H, Sun W, Zhang C, Zhou C, Fang C-J and Yan C-H 2009 *Chem. Eur. J.* **15** 8717